

Chapter 7

Transition Radiation from Electron Bunches

7.1 Radiation from Electron Bunches

The total electromagnetic radiation emitted from a bunch of N electrons is the sum of the radiation emitted from each individual electron in the bunch with an appropriated phase factor. The theoretical discussion of radiation from an electron bunch in this chapter will be simplified to the longitudinal coordinate since we are interesting in only longitudinal electron bunch length. However, the result can be extended to a three dimensional bunch.

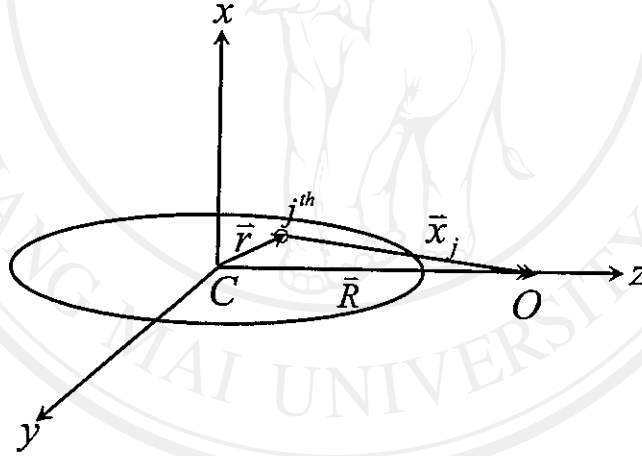


Figure 7.1. Schematic model of an electron bunch of N electrons showing the coordinate of the j^{th} electron referring to the center of the bunch (C) and the observation point (O).

An electromagnetic radiation field at angular frequency ω from a single electron can be expressed like $\vec{E}_j(\omega) = \vec{E}_{0j} e^{i(\omega t - \vec{k}_j \cdot \vec{r})}$, where \vec{r}_j is the position vector from center of the bunch to the j^{th} electron and $\vec{k}_j = k \hat{n}_j = (\frac{\omega}{c}) \hat{n}_j$ is the wave number vector of the electric field from the j^{th} electron with the direction vector \hat{n}_j to the observation point. As indicated in Fig.(7.1), \vec{x}_j is the vector from the j^{th} electron to the observation point (O) and it can be expressed as $\vec{x}_j \equiv x_j \hat{n}_j = \vec{R} + \vec{r}_j$. The total radiation field from a bunch of N electrons at a frequency ω can be written

as the sum of single radiation fields from all electrons in the bunch as

$$\vec{E}(\omega) = \sum_{j=1}^N \vec{E}_j(\omega) = \sum_{j=1}^N \vec{E}_{0j}(\omega) e^{i(\omega t - \vec{k}_j \cdot \vec{r}_j)}. \quad (7.1)$$

By use of a far-field approximation as the observation vector \vec{R} from the bunch center (O) is very large compared to the position vector \vec{r}_j ($\vec{R} \gg \vec{r}_j$), it can be approximated that the unit vector $\hat{n}_j \approx \hat{n}$ and $\vec{k}_j = k\hat{n}_j \approx k\hat{n}$. This leads to another approximation of the radiation field of individual electrons as $\vec{E}_{0j}(\omega) \approx \vec{E}_0(\omega)$, where $\vec{E}_0(\omega)$ is the radiation field at frequency ω for an electron at the bunch center. Hence, the total emitted field in (7.1) becomes

$$\vec{E}(\omega) = \sum_{j=1}^N \vec{E}_0(\omega) e^{i(\omega t - k\hat{n} \cdot \vec{r}_j)}. \quad (7.2)$$

The total spectral radiation intensity $I(\omega)$ is proportional to the square of the absolute value of the total spectral fields $I(\omega) \propto |\vec{E}(\omega)|^2$. By assuming that all electrons in the bunch have the same energy, the total radiation intensity emitted by the electron bunch can be written as

$$I(\omega) \approx \left| \sum_{j=1}^N \vec{E}_0(\omega) e^{i(\omega t - k\hat{n} \cdot \vec{r}_j)} \right|^2. \quad (7.3)$$

To simplify the radiation intensity in (7.3) to be in one dimensional coordinate along the longitudinal direction, the three dimensional phase difference ($k\hat{n} \cdot \vec{r}_j$) in the exponent of the electromagnetic field can be replaced by the phase difference φ and the total radiation intensity of the electron bunch

$$I(\omega) \approx \left| \sum_{j=1}^N \vec{E}_0(\omega) e^{i(\omega t + \delta\varphi_j)} \right|^2 = N |\vec{E}_0(\omega)|^2 + |\vec{E}_0(\omega)|^2 \sum_{j,k=1}^N (j \neq k) e^{i(\delta\varphi_j - \delta\varphi_k)}. \quad (7.4)$$

The exponential term in (7.4) can be transformed into an electron bunch length term in the longitudinal z -direction by $\delta z = \lambda(\delta\varphi_j - \delta\varphi_k)/2\pi$, where λ is the wavelength of the radiation at frequency ω which corresponds to the wave number k by $\lambda/2\pi = c/\omega = 1/k$.

For a case of a short electron bunch length compared to the radiation wavelength, $\delta z \ll \lambda$ ($\delta\varphi_j \approx \delta\varphi_k$), the total radiation intensity in (7.4) becomes

$$I(\omega) = N |\vec{E}_0(\omega)|^2 + N(N-1) |\vec{E}_0(\omega)|^2. \quad (7.5)$$

Since the single-electron field emission $\vec{E}_0(\omega)$ relates to a radiation intensity $I_e(\omega)$ from a single electron as $I_e(\omega) \approx |\vec{E}_0(\omega)|^2$, the total radiation intensity emitted from all electrons in the bunch can be written as

$$I(\omega) = NI_e(\omega) + N(N-1)I_e(\omega). \quad (7.6)$$

Hence, for the radiation with wavelength longer than the electron bunch length, the electromagnetic fields emitting from all electrons are at about the same phase, and they add up coherently scaling with the number of electron squared as

$$I_{coherent}(\omega) = N^2 I_e(\omega). \quad (7.7)$$

On the other hand, for a radiation wavelength shorter than the electron bunch length, $\lambda \ll \delta z$ or $(\delta\varphi_j - \delta\varphi_k) \gg \lambda$, fields emitted from all electrons in the bunch are at random phase spreading over more than 2π . The second term in (7.4) vanishes due to cancellation of the random phase and the total intensity for this case leads to the incoherent radiation as

$$I_{incoherent}(\omega) = N |\vec{E}_0(\omega)|^2 = NI_e(\omega). \quad (7.8)$$

It can be summarized from (7.7) and (7.8) that coherent radiation is N time more intense than incoherent radiation. This coherent enhancement of electron bunch was originally predicted by Nodvick and Saxon in 1954 [63]. Typically, in our electron beam there are about $10^8 - 10^9$ electrons in an electron bunch, resulting in different intensity of the coherent and the incoherent part by about 8–9 orders of magnitude. This agrees well with the intense FIR coherent radiation for the electron bunch length of the sub-picosecond range. Figure 7.2 shows the model of the radiation from short electron bunch (top) and from long electron bunch (bottom) compared to the radiation wavelength.

Considering the transition regime of the two limits between the coherent and incoherent radiation fields, where the electron bunch length is about equal to the radiation wavelength, $\delta z \approx \lambda$ or $(\delta\varphi_j - \delta\varphi_k) \approx 2\pi$. Then the total radiation intensity in (7.5) may be written in terms of individual electron intensity $I_e(\omega)$ as

$$I(\omega) = NI_e(\omega) + N(N-1)I_e(\omega)f(\omega), \quad (7.9)$$

where the factor $f(\omega)$ is called the *bunch form factor* that depends greatly on the electron distribution in the bunch. It can be concluded from (7.9) that between

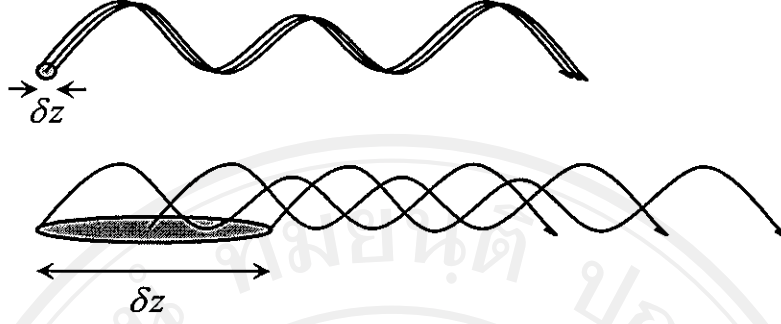


Figure 7.2. Schematic model of the radiation from short electron bunch (top) and long electron bunch (bottom) compared to the radiation wavelength.

the two limits of $\delta z \gg \lambda$ and $\delta z \ll \lambda$, the total intensity depends on the number of electrons in the bunch and positions of individual electrons.

Typically, an electron bunch contains a large number of electrons in a very small volume in the order of mm^3 . We can describe positions and distribution of electrons in the bunch by using the electron continuous distribution, which is the probability of finding electrons at the position vector \vec{r} . Assume that electrons in the volume element $d^3\vec{r}$ located at the position vector \vec{r} . The bunch distribution $S(\vec{r})$ satisfies the normalized probability function condition for three dimensional bunch form factor as

$$f(\omega) \equiv \left| \int e^{ik\hat{n}\cdot\vec{r}} S(\vec{r}) d^3\vec{r} \right|^2. \quad (7.10)$$

If we assume that the transverse and longitudinal distribution are independent, we can express the three dimensional bunch distribution by $S(\vec{r}) = S(x, y, z) \equiv S_1(x, y)S_2(z)$ for cartesian coordinates or $S(\vec{r}) = S(\rho, \theta, z) \equiv S_1(\rho, \theta)S_2(z)$ for cylindrical coordinates. Since we are interesting only in the longitudinal bunch length lets assume that all electrons in the bunch are distributed azimuthally symmetric about the direction of the beam propagation along the z-direction. Then, the contribution from the transverse bunch distribution become unity for all frequencies because $\int_{-\infty}^{\infty} \int_{-\infty}^{\infty} S_1(x, y) dx dy = 1$ or $\int_0^{\infty} \int_0^{2\pi} S_1(\rho, \theta) d\rho d\theta = 1$ and the bunch form factor will be reduced to be the simplest form of the longitudinal bunch distribution $S_z(z)$. Then, the bunch form factor in one dimension along the longitudinal direction can be written as

$$f(\omega) \equiv \left| \int e^{ikz} S(z) dz \right|^2 = \left| \int e^{2\pi i(\omega/c)z} S(z) dz \right|^2, \quad (7.11)$$

and the one-dimensional total radiation intensity becomes

$$I(\omega) = \left| \int N \vec{E}_0(\omega) e^{ikz} S(z) dz \right|^2. \quad (7.12)$$

The enhancement of coherent radiation over incoherent radiation can be seen in (7.11) and (7.12) that at low frequency where $\omega \rightarrow 0$ and the electron bunch length is much shorter compared to the radiation wavelength, the form factor is close to unity and the coherent contribution will be N times larger than the incoherent part. On the other hand, at high frequencies, where the radiation wavelength approaches zero, the form factor vanishes leaving only the incoherent contribution. From this coherent enhancement it becomes clear why coherent radiation can be used to measure the electron bunch length, where the incoherent radiation does not have the bunch form factor containing the information of the bunch distribution. The bunch form factor contains information on the longitudinal electron distribution and measurement of the coherent radiation spectrum (intensity vs. frequency) gives immediately by a Fourier transform the bunch length or vice versa.

To calculate the radiation intensity in (7.9) and (7.11), one needs to derive the Fourier transform of the normalized bunch distribution. Typical example of the bunch distribution is the uniform distribution, where the bunch is symmetric about the z -direction with rectangular longitudinal distribution of length $2\sigma_z$ where electrons only distribute along $z = -\sigma_z$ to $z = +\sigma_z$ as shown in Fig.7.3(a) and described by

$$S(z) = \frac{1}{2\sigma_z}, \text{ for } |z| \leq \sigma_z. \quad (7.13)$$

The bunch form factor is then

$$f(\omega) = \left| \int_{-\sigma_z}^{+\sigma_z} e^{ikz} \left(\frac{1}{2\sigma_z} \right) dz \right|^2 = \left[\frac{\sin(k\sigma_z)}{\sigma_z k} \right]^2 = \left[\frac{\sin(\omega\sigma_z/c)}{\omega\sigma_z/c} \right]^2, \quad (7.14)$$

where $k = \omega/c$. Another typical example is a Gaussian distribution, which is a good representation of the longitudinal distribution for most electron bunches. A Gaussian longitudinal distribution of the equivalent length $\sqrt{2\pi}\sigma_z$ as shown in Fig.7.3(b) is defined by

$$S(z) = \frac{1}{\sqrt{2\pi}\sigma_z} e^{-z^2/2\sigma_z^2}, \quad (7.15)$$

and the bunch form factor can be evaluated as

$$f(\omega) = \left| \int_{-\infty}^{\infty} e^{ikz} \frac{e^{-z^2/2\sigma_z^2}}{\sqrt{2\pi}\sigma_z} dz \right|^2 = \left[e^{-\frac{k^2\sigma_z^2}{2}} \right]^2 = e^{-(\omega\sigma_z/c)^2}. \quad (7.16)$$

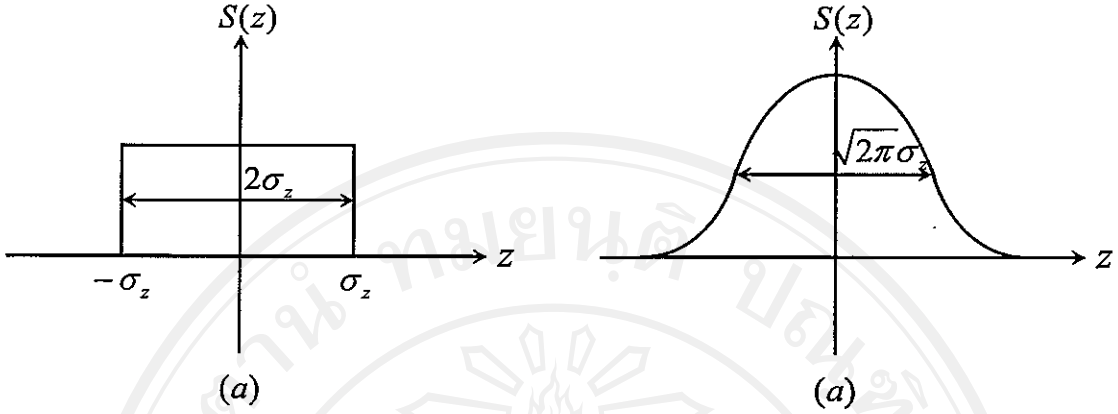


Figure 7.3. Typical bunch distributions: (a). a uniform distribution with rectangular longitudinal distribution of length $2\sigma_z$ and (b). a Gaussian distribution with the FWHM of length $\sqrt{2\pi}\sigma_z$.

In reality, when the electron bunch radiates, the radiation is emitted from a three dimensional source. The longitudinal contribution of the form factor represents the spectral degree of temporal coherence and the transverse contribution of the form factor plays an important role to the spectral degree of spatial coherence. The concepts of temporal and spatial coherence are important in discussion about the phase characteristics of the radiation from electron bunches. The temporal coherence describes the correlation between signals observed at different moments in time while the spatial coherence is described as a function of distance, which is correlated between signals at difference points in space. Theoretical derivation of the bunch form factor for three dimensional distribution can be found in reference [18] and [64].

7.2 Transition Radiation

When electron passes through an interface between two media of different dielectric constants, it emits electromagnetic fields due to the sudden transition of the dielectric constant of the media along the electron path and causes a discontinuity in the electric fields at the interface. This electromagnetic radiation is called *transition radiation (TR)* due to its property that is emitted at the media transition. The transition radiation was first predicted by Ginsburg and Frank [65]. Lets consider a simple picture of the transition radiation from an electron

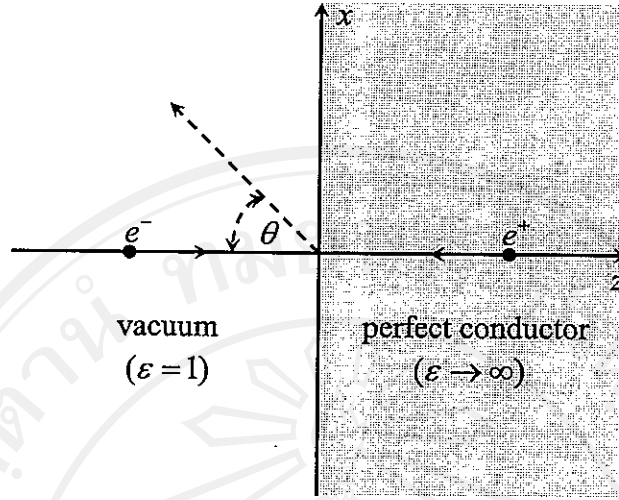


Figure 7.4. The two-charged-particle collision problem represents the transition radiation (dashed-arrow) emitted when an electron moves from vacuum to a perfect conductor in a direction normal to the interface [18].

of constant velocity travels in a direction normal to the interface between vacuum with the dielectric constant of unity ($\epsilon = 1$) and a perfect conductor with infinite dielectric constant ($\epsilon \rightarrow \infty$). Since the surface boundary is a perfect conductor, the method of image charge can be applied to this problem, which introduces a positive image charge of the electron located on the other side of the surface boundary at the same distance as the electron (as shown in Fig.7.4). Then, the problem reduces to a simple two-charged-particle collision system. The radiation of frequency ω is emitted when the two charges collide with a very short collision time ($\tau \ll 2\pi\omega$) or we can say that their velocities change instantaneously. Then, the radiation energy W emitted in the frequency range $d\omega$ into a solid angle $d\Omega$ may be written as [18]

$$\frac{dW}{d\omega d\Omega} = \frac{1}{4\pi^2 c^3} \left[\sum_j q_j \left(\frac{\vec{v}_{j,2} \times \vec{n}}{1 - \vec{n} \cdot \vec{\beta}_{j,2}} - \frac{\vec{v}_{j,1} \times \vec{n}}{1 - \vec{n} \cdot \vec{\beta}_{j,1}} \right) \right]^2, \quad (7.17)$$

where q_j is the charge of j^{th} particle, $\vec{v}_{j,1}$ is the initial velocity before the sudden change, $\vec{v}_{j,2}$ is the final velocity after the sudden change, \vec{n} is the unit vector in the emitted radiation direction and $\vec{\beta} = \vec{v}/c$. Let's consider the electron of charge e moving with velocity \vec{v} collides with a position of charge $-e$ moving with a velocity $-\vec{v}$ at the interface. Then, the components $\vec{v}_{1,2} = \vec{v}_{2,2} = 0$, $\vec{v}_{1,1} = \vec{v}$ and $\vec{v}_{2,1} = -\vec{v}$. The radiation energy per unit angular frequency per unit solid angle

for the backward transition radiation becomes

$$\frac{dW}{d\omega d\Omega} = \frac{e^2 \beta^2 \sin^2 \theta}{\pi^2 c (1 - \beta^2 \cos^2 \theta)^2}, \quad (7.18)$$

where θ is the angle between $-\vec{v}$ and the normal direction \vec{n} to the interface (emitted angle). Results in (7.18) can be extended to a more general case of an electron moving across an interface between a vacuum and a finite dielectrics constant ϵ in the normal direction and the backward transition radiation angular spectral energy density will be

$$\frac{dW}{d\omega d\Omega} = \frac{e^2 \beta^2 \sin^2 \theta \cos^2 \theta}{\pi^2 c (1 - \beta^2 \cos^2 \theta)^2} \left| \frac{(\epsilon - 1)(1 - \beta^2 + \beta \sqrt{\epsilon - \sin^2 \theta})}{(1 + \beta \sqrt{\epsilon - \sin^2 \theta})(\epsilon \cos \theta + \sqrt{\epsilon - \sin^2 \theta})} \right|. \quad (7.19)$$

Equation (7.19) will be reduced to be (7.18) when the dielectric constant is set for the perfect conductor as $\epsilon \rightarrow \infty$. It can be seen from (7.18) and (7.19) that the spectral energy depends on velocity (β) and the emitted angle θ .

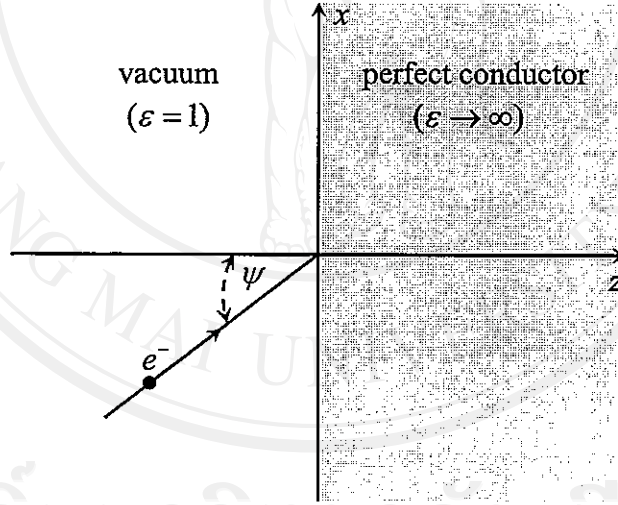


Figure 7.5. An electron moves from vacuum to a perfect conductor in at an incident angle ψ with respect to the z -axis.

Since in our experimental setup the transition radiation will be generated when an electron beam collides on the 45° tilted aluminum foil the transition radiation spectrum for oblique incidence will be introduced. Lets consider an electron moving from vacuum ($\epsilon = 1$) to aluminum foil with an incident angle of ψ as shown in Fig.7.5. To simplify the problem let us consider that the aluminum foil is a perfect conductor since its dielectric constant is much more than that of vacuum in the far infrared regime [18] and we can set its dielectric constant $\epsilon \rightarrow \infty$. For

oblique incident, the backward transition radiation may have two polarizations: a parallel polarization (W_{\parallel}) with electric field lies in the radiation plane and a perpendicular polarization (W_{\perp}) with electric field perpendicular to the radiation plane [18]. Hence, the total backward transition radiation intensity including both planes becomes

$$\frac{dW}{d\omega d\Omega} = \frac{dW_{\parallel}}{d\omega d\Omega} + \frac{dW_{\perp}}{d\omega d\Omega}, \quad (7.20)$$

for transition from vacuum to a perfect conductor medium, the parallel and perpendicular polarization are

$$\frac{dW_{\parallel}}{d\omega d\Omega} = \frac{e^2 \beta^2 \cos^2 \psi}{\pi^2 c} \left[\frac{\sin \theta - \beta \cos \phi \sin \psi}{(1 - \beta \sin \theta \cos \phi \sin \psi)^2 - \beta^2 \cos^2 \theta \cos^2 \psi} \right]^2, \quad (7.21)$$

$$\frac{dW_{\perp}}{d\omega d\Omega} = \frac{e^2 \beta^2 \cos^2 \psi}{\pi^2 c} \left[\frac{\beta \cos \theta \sin \phi \sin \psi}{(1 - \beta \sin \theta \cos \phi \sin \psi)^2 - \beta^2 \cos^2 \theta \cos^2 \psi} \right]^2, \quad (7.22)$$

where θ is the angle between the emitted radiation direction \vec{n} and the $-z$ axis while ϕ is the azimuthal angle defined in the xy -plane with respect to the $-x$ axis and ψ is the incident angle of electron with respect to the $-z$ axis. For our case where the electron collides with the aluminum surface at 45° ($\psi = 45^\circ$), the parallel and perpendicular polarization becomes

$$\frac{dW_{\parallel}}{d\omega d\Omega} = \frac{e^2 \beta^2}{2\pi^2 c} \left[\frac{2 \sin \theta - \sqrt{2} \beta \cos \phi}{(\sqrt{2} - \beta \sin \theta \cos \phi)^2 - \beta^2 \cos^2 \theta} \right]^2, \quad (7.23)$$

$$\frac{dW_{\perp}}{d\omega d\Omega} = \frac{e^2 \beta^2}{2\pi^2 c} \left[\frac{\sqrt{2} \beta \cos \theta \sin \phi}{(\sqrt{2} - \beta \sin \theta \cos \phi)^2 - \beta^2 \cos^2 \theta} \right]^2. \quad (7.24)$$

7.3 Transition Radiation Acceptance

The angular spectral distribution of the transition radiation in case of normal incidence can be explained by (7.18) and it reveals that there is no radiation in the forward direction since $\theta = 0$ and it is azimuthally symmetric since it has no ϕ dependence. The maximum radiation intensity is $e^2 \gamma^2 / (4\pi^2 c)$ at $\sin \theta = 1/(\beta\gamma)$, where γ is the Lorentz factor with $\gamma = (\sqrt{1 - \beta^2})^{-1}$. In case of relativistic electrons ($\beta \rightarrow 1$ and $\gamma \gg 1$) we can approximate $\sin \theta \approx \theta$ and the maximum radiation intensity can be obtained at $\theta \approx \pm 1/\gamma$. It can be concluded

that the radiation distribution becomes more collimated for higher electron energies. A linear accelerator was installed for post acceleration to higher collimation since a 15 MeV electron has the maximum intensity at an expected angle of ± 34.1 mrad compared to ± 170 mrad for a 3 MeV electron beam from the RF-gun. Thus, adding the linac to accelerate electron to about 15 MeV after bunch compression is a reasonable way to generate a more confined beam of transition radiation.

The angular distribution in the case of oblique incidence has an azimuthal asymmetry since it has the azimuthal ϕ dependence. This leads to the maximum radiation intensity for the case of 45° incidence to be located at an angle larger than $\pm 1/\gamma$. However, for the highly relativistic electron like in our case the angular distribution asymmetry vanishes. Hence, we can use the radiation distribution for normal incidence to consider the transition radiation in our case [18]. Generally, much of the transition radiation is emitted larger than its maximum intensity angle of $1/\gamma$ due to its angular distribution property. To collect the radiation in experiments, an acceptance angle must be considered. The total radiation emitted within an acceptance angle θ_a can be obtained by integrating the angular distribution in (7.18) over solid angles to the limit determined by the acceptance angle as

$$\frac{dW}{d\omega}(\theta_a) = \int_0^{2\pi} \int_0^{\theta_a} \frac{dW}{d\omega d\Omega} \sin\theta d\theta d\phi. \quad (7.25)$$

Lets consider only the backward radiation into the left half space in the vacuum side in Fig.7.4, the integration of the radiation energy over the left half space becomes

$$\frac{dW}{d\omega} = \int_0^{2\pi} \int_0^{\pi/2} \frac{dW}{d\omega d\Omega} \sin\theta d\theta d\phi = \frac{e^2}{2\pi c} \left[\frac{1+\beta^2}{\beta} \ln\left(\frac{1+\beta}{1-\beta}\right) - 2 \right]. \quad (7.26)$$

It can be seen in (7.26) that for highly relativistic electrons with $\beta \rightarrow 1$ and $\gamma \gg 1$, the term $(1-\beta)^{-1} \rightarrow 2\gamma^2$ and the total radiation energy in the frequency range $d\omega$ for high energy electrons is proportional to $\ln\gamma$. The radiation collection efficiency depends greatly on the acceptance angle θ_a which is specified by an experimental setup. In our experiments, so far the electron beam can be accelerated to reach about 11 MeV leading to the maximum acceptance angle for the transition radiation at about $34/\gamma$.

7.4 Coherent Transition Radiation Spectrum

According to the fact that at wavelengths much longer than the bunch length, radiation fields add up coherently and a shorter bunch length provides a broader spectrum. The radiation brightness versus wave number of far-infrared radiation (FIR) spectrum in Fig.7.6 shows that sub-picosecond electron bunches can provide broadband radiation in the far-infrared regime with intensity much higher than black body radiation and synchrotron radiation and shorter bunches provide broader spectrum.

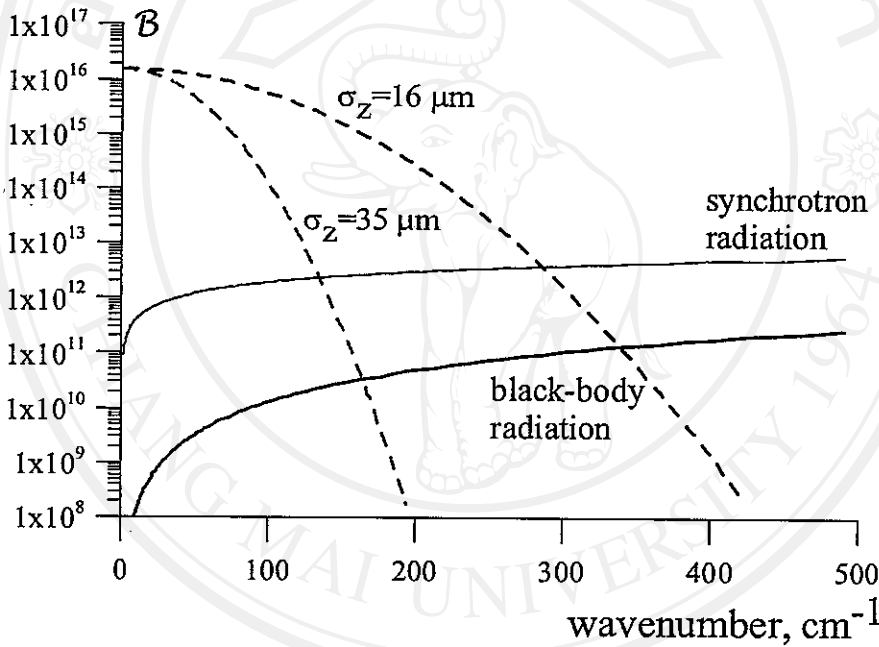


Figure 7.6. Radiation brightness B (ph/s/mm²/100%BW) vs. wave number for coherent transition radiation for 16 μm and 35 μm compared to synchrotron radiation and black body radiation.

Comparison of the electron bunch length of about 120 fs (35 μs) produced at SUNSHINE facility [18] and the expected bunch length of about 53 fs (16 μs) at SURIYA facility is illustrated in Fig.7.6. It reveals that the shorter bunch of about a factor of two at the SURIYA facility gives a spectrum twice as broad than the SUNSHINE bunch. With electron bunch length of about 53 fs the far infrared radiation from transition radiation is expected to cover the wave number range from 5 cm^{-1} to 400 cm^{-1} . The intensity is greater by 4 to 8 orders of magnitude

compared to a conventional black body sources and by 2 or 3 order of magnitude greater than synchrotron light sources.

7.5 Transition Radiation Generation and Observation

Far-infrared radiation is generated by transition radiation method. A radiator made of aluminum foil (Al-foil) is placed in the electron path, representing transition between vacuum and Al-foil. At SURIYA, the transition radiation station where the measurements were taken for this thesis was located at about 2 m from the linac exit (see Fig.5.1). A $25.4\text{-}\mu\text{m}$ -thick aluminum foil of 24 mm diameter was support on an aluminum ring using the drumhead stretching technique. The radiator is tilted by 45° facing the electron beam direction. The backward transition radiation is emitted perpendicular to the beam axis and transmits through a high density polyethylene (HDPE) window of 1.25-mm-thick and 32-mm diameter. The polyethylene window allows 87% transmission of the radiation in the far-infrared regime [66]. A 14-cm long copper light cone is used to collect the radiation into a room-temperature pyroelectric detector. A cross-sectional diagram of the experimental set up for measuring the transition radiation is shown in Fig.7.7.

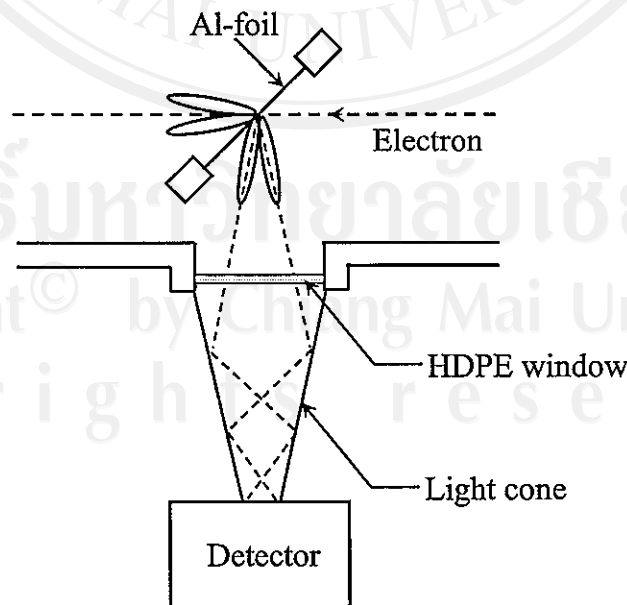


Figure 7.7. Transition radiation measurement setup.

The far-infrared detector consists of a Molelectron P1-65 LiTaO₃ pyroelectric sensor of 5-mm diameter and a pre-amplifier. Its sensitivity is uniform over a spectral range from visible light to millimeter waves which covers more than the full range of the expected transition radiation. The detector was calibrated by using a Scientech thermopile power meter which gives an energy responsivity of 0.97 mJ/V [67].

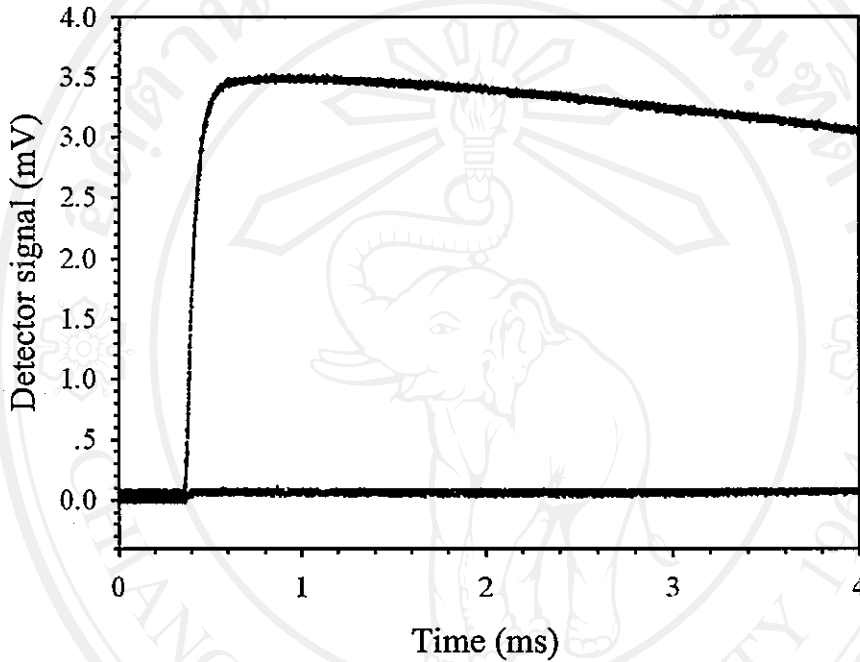


Figure 7.8. The transition radiation (TR) signal at SURIYA facility (March 21, 2006). The top curve shows the TR signal observed with the pyroelectric detector and the bottom curve shows the TR signal when an Al-foil is placed between the source and the detector.

Far-infrared radiation signal from short electron bunches generating as transition radiation was observed and verified for the first time at SURIYA on March 21, 2006. We verified whether the radiation was indeed far-infrared radiation by placing an Al-foil at the entrance of the detector. Aluminum foil is well known as an excellent far-infrared radiant barrier since it has a low emissivity of 0.05. It eliminates 95% of the radiation transfer by reflection [68]. The measurement result shows that almost 100% of the detector signal vanishes after the detector was blocked by the Al-foil as shown in Fig.7.8. This is verification that the detector signal that we observed is indeed far-infrared radiation and not high energy ionizing radiation. The detector signal was observed at 3.5 mV results in

a total measured energy of the transition radiation from each macropulse of $3.4 \mu\text{J}$ or a peak power of 4.2 W .



ลิขสิทธิ์มหาวิทยาลัยเชียงใหม่
Copyright© by Chiang Mai University
All rights reserved